An Active Learning Pipeline for Biomedical Image Instance Segmentation with Minimal Human Intervention

Shuo Zhao¹, Yu Zhou^{1,2}, Jianxu Chen¹,

¹Leibniz-Institut für Analytische Wissenschaften - ISAS - e.V. ²Faculty of Computer Science, Ruhr University Bochum jianxu.chen@isas.de

Abstract. Biomedical image segmentation is critical for precise structure delineation and downstream analysis. Traditional methods often struggle with noisy data, while deep learning models such as U-Net have set new benchmarks in segmentation performance. nnU-Net further automates model configuration, making it adaptable across datasets without extensive tuning. However, it requires a substantial amount of annotated data for cross-validation, posing a challenge when only raw images but no labels are available. Large foundation models offer zero-shot generalizability, but may underperform on specific datasets with unique characteristics, limiting their direct use for analysis. This work addresses these bottlenecks by proposing a data-centric AI workflow that leverages active learning and pseudo-labeling to combine the strengths of traditional neural networks and large foundation models while minimizing human intervention. The pipeline starts by generating pseudo-labels from a foundation model, which are then used for nnU-Net's self-configuration. Subsequently, a representative core-set is selected for minimal manual annotation, enabling effective fine-tuning of the nnU-Net model. This approach significantly reduces the need for manual annotations while maintaining competitive performance, providing an accessible solution for biomedical researchers to apply state-of-the-art AI techniques in their segmentation tasks. The code is available at https://github.com/MMV-Lab/AL_BioMed_img_seg.

1 Introduction

Image segmentation is crucial in biomedical image analysis, as it allows precise delineation of structures, which could be used for downstream quantification and modeling. The field of biomedical image segmentation has evolved significantly with deep learning techniques. Although traditional methods such as thresholding or graph-based methods were foundational, they often yield much worse performance on challenging tasks (e.g., noisy data) compared to deep learning-based approaches such as U-Net [1].

Traditional neural networks such as nnU-Net further improved this by automating model configuration for different segmentation tasks [2], which has become a strong baseline method in segmentation benchmarks. nnU-Net can adapt to various biomedical imaging datasets without extensive manual tuning, effectively overcoming the challenges associated with manual network design and configuration. Empirical selection requires a complete training set or sufficient data for five-fold cross-validation. However, obtaining labeled data for nnU-Net, especially in 3D image analysis, is time-consuming and requires knowledge and expertise. In practice, data often has no labels.

2 Zhao, Zhou & Chen

Unsupervised active learning advances core-set selection for efficient training and lower annotation costs but faces challenges in feature selection and initialization. [3].

Meanwhile, different network architectures, such as transformer-based models and hybrid models combining convolutional neural networks (CNNs) with transformers, have also been proposed to improve segmentation by capturing long-range dependencies in images [7]. Recent developments in large foundation models, such as SAM [8], SAM2 [9], cellSAM [4], microSAM [10], medSAM [11], have further advanced the field toward generalist models for biomedical image segmentation. However, large foundation models often struggle with specific datasets, such as unique tissue environments or drug-treated cells, limiting their effectiveness in direct downstream analysis.

We address the two bottlenecks with an active learning pipeline based on the idea of data-centric AI to solve these two bottlenecks, which focuses on data quality and diversity rather than model complexity [12]. This pipeline combines traditional neural networks and large foundation models with minimal human input. A 3D mitochondrial segmentation [13] was used as an example. Pseudo-labels generated from a foundation model for raw images can be used to create a training set for self-configuration and pre-training. This approach enables nnUNet to work with unlabeled images. A core-set is a small, representative subset that approximates the properties of the full dataset. Then a core-set was selected for manual annotation and fine-tuning the pre-rained nnUnet, leading to a robust model with minimal manual effort. It is worth mentioning that this paper focuses on an active learning pipeline to address key bottlenecks in traditional neural networks and large foundation models. So we focus on demonstrating and validating the effectiveness of this pipeline rather than competing on leaderboards.

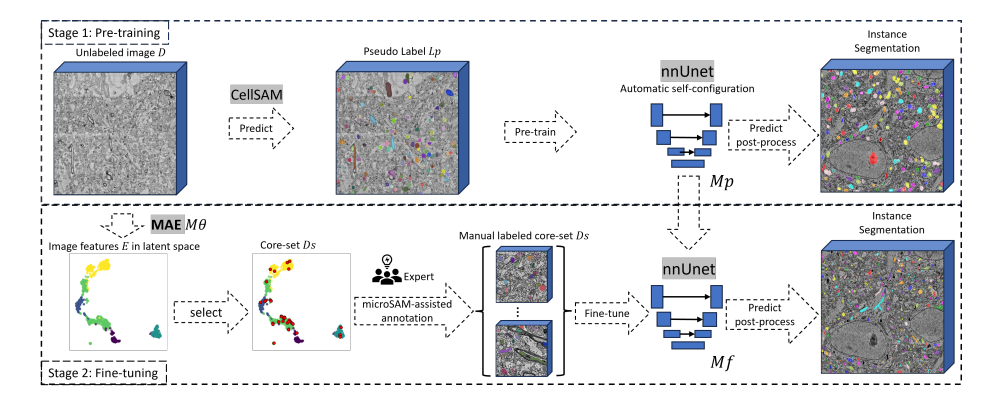


Fig. 1. An active learning pipeline for 3D unlabeled biomedical image instance segmentation. This pipeline consists of two main stages: Pre-training and Fine-tuning. Stage 1: Pre-training. Pseudo-labels were generated from CellSAM [4] for unlabeled raw images, forming a training set for nnU-Net to run self-configuration and pre-training. Stage 2: Fine-tuning. Unlabeled images were mapped into a latent space to select a representative core-set [5], using features from a pre-trained foundation model MAE [6] via self-supervised learning. The pre-trained nnUnet model was fine-tuned by using minimal microSAM-assisted annotations.

2 Materials and methods

2.1 Methods

The proposed pipeline (Fig. 1) consists of two main stages: pre-training and fine-tuning. Stage 1: Pre-training. To enable nnU-Net M_p to run self-configuration and pre-training, avoiding manual design, pseudo-labels L_p were generated from CellSAM [4] for unlabeled raw images D. Then D and L_p formed a train set for nnU-Net M_p .

Stage 2: Fine-tuning. The selected core-set D_s and its manual label were used to fine-tune the pre-trained nnU-Net M_p . We selected raw images based on their latent space features. An MAE model M_θ using U-net architecture was trained with unlabeled images D via self-supervised learning. According to $E = M_\theta(D)$, D were mapped into a latent space as the features E. Pre-trained MAE models excel in scalability, speed, and feature extraction, outperforming supervised models [14]. According to $d = 1 - E \cdot E^T$, a cosine distance matrix d was computed between features E.

Unlabeled images D consists of a selected core-set D_s [5] and unselected set D_u . The core-set selection algorithm, initialization, k (k = 3) samples were selected randomly from D_u . Then, each sample S in D_u was traversed, find the minimum distance $d_{\min}(S, D_s)$ for each S to D_s . Then the sample S in D_u with the maximum d_{\min} was selected to D_s . We repeated this process, and finally get a core-set D_s of size N.

The unlable selected core-set D_s was checked and annotated by experts with minimal manual effort, assisted by microSAM [10]. Then D_s and manual labels were used to fine-tune the nnU-Net M_p , resulting in M_f . Connected components were applied to make instance segmentation as in MitoEM Challenge [13].

2.2 Validation on the 3D unlabeled dataset MitoEM

The MitoEM Grand Challenge [13] is an international competition focused on segmenting mitochondria in electron microscopy images. The 3D MitoEM dataset [15] contains two high-resolution volumes, each measuring $30 \times 30 \times 30 \mu m$ with voxel dimensions of $1000 \times 4096 \times 4096$ at $30 \times 8 \times 8$ nm resolution. Each volume is divided into training (400 slices), validation (100 slices), and test (500 slices) sets. Although it has ground truth (GT), we assume no GT is available for training, as in real-world tasks.

3 Experiment

All experiments were run on 8 NVIDIA A100 GPUs (40GB). For fair experiments, we simply adopt the hyperparameters in the original nnUnet codebase for training.

For dataset preprocessing, train and test sets were padded and cropped into 1024 patches ($32 \times 512 \times 512$). 2D pseudo-labels were generated by CellSAM and combined into 3D patch labels. nnU-Net was pre-trained and fine-tuned automatically. MAE models were trained on 1000 raw 2D images with a 0.75 mask ratio for 400 epochs. Then the pre-trained encoders were used to extract image features. Patches were selected by the core-set selection algorithm (k = 3). Core-sets were annotated by microSAM with the vit_b model. Fine-tuned models segmented the test set, with post-processing

4 Zhao, Zhou & Chen

Tab. 1. Evaluation metrics for fine-tuning with different core-set sizes. Where the 1024 core-set represents the full manually labeled set. Each double row displays the score and percentage of the full set score. *Bold* text highlights when the score first surpasses 90% of the full set performance.

Core-set Size	0	8	16	32	64	128	256	512	1024
Percentage (%)	(0.00)	(0.78)	(1.56)	(3.13)	(6.25)	(12.50)	(25.00)	(50.00)	(100.00)
F1 Score	0.4025	0.4462	0.5297	0.5630	0.5884	0.6003	0.6011	0.6294	0.6350
Percentage (%)	63.38	70.26	83.41	88.66	92.65	94.53	94.65	99.12	100.00
Accuracy	0.2521	0.2882	0.3603	0.3918	0.4170	0.4291	0.4298	0.4593	0.4652
Percentage (%)	54.19	61.95	77.45	84.22	89.63	92.23	92.39	98.72	100.00
Panoptic	0.3628	0.3962	0.4723	0.5038	0.5284	0.5405	0.5421	0.5689	0.5750
Percentage (%)	63.09	68.90	82.13	87.61	91.89	93.99	94.26	98.93	100.00
Precision	0.2824	0.3300	0.4181	0.4599	0.4926	0.5045	0.5058	0.5411	0.5554
Percentage (%)	50.85	59.42	75.29	82.81	88.70	90.85	91.08	97.43	100.00

and evaluation following the MitoEM Challenge [13]. For ablation experiments, we compared nnU-Net models trained on the core-set with those pre-trained on pseudo-labels. We also assessed the impact of various core-set sizes, from 8 to 1024 samples.

4 Results

We observed that *simply relying on pseudo-labels from large foundation models may be insufficient*. As shown in Fig. 2, pseudo-labels (Fig. 2a) closely resemble the manual labels in (Fig. 2b). However, yellow arrows highlight labeling errors, e.g., imprecise boundaries and false negatives. The white arrows indicate that, compared to GT (Fig. 2f), the segmentation after pre-training (Fig. 2c) detects mitochondria but has inaccuracies. *The selected core-sets are reasonable and effective*. Fig. 4 shows the latent space distribution of image features, with red points marking diverse, representative patches that enhance information density. *Fine-tuning with the selected core-set is effective*. As shown in Fig. 2, fine-tuning with 12.5% and 100% manual labels (Fig. 2d, Fig. 2e) improves segmentations closer to the GT (Fig. 2f). Fig. 3 and Tab. 1 show fine-tuning results with different core-set sizes. Tab. 1 highlights that F1 score and Panoptic metrics surpassed 90% at 6.25% (64 samples), and Accuracy and Precision at 12.5% (128

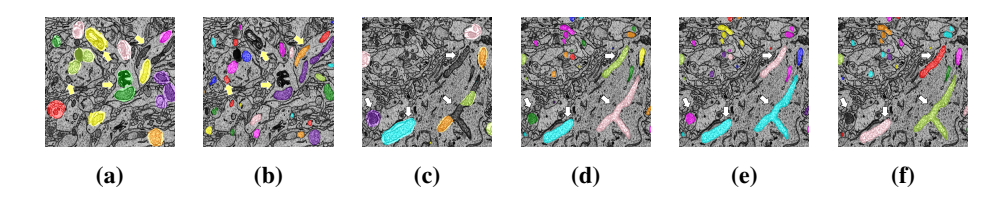


Fig. 2. Labels for the train set: (a) pseudo-labels from cellSAM and (b) manual labels. Segmentations for the test set: (c) pre-trained with pseudo-labels, (d) fine-tuned with 12.5% manual labels, (e) fine-tuned with 100% manual labels, and (f) GT. Yellow arrows in (a) and (b) show differences between pseudo and manual labels, while white arrows in (c)–(f) highlight discrepancies between segmentations and the GT.

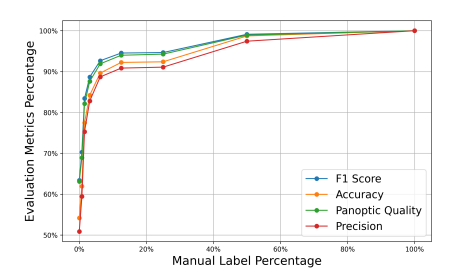


Fig. 3. Instance segmentation metrics: The X-axis shows manual annotation percentage, and the Y-axis shows performance relative to full labels. As manual annotations increase, the model's performance improves. At about 12.5% annotations, the model achieves 90% of the full annotation performance.

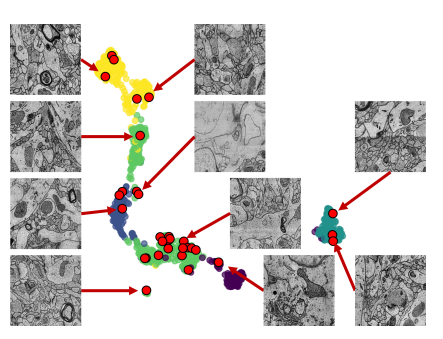


Fig. 4. Examples of patches in the selected coreset. The plot visualizes the latent features of all patches in latent space after UMAP dimensionality reduction. Red dots represent the selected image patches. The selected patches cover a wide range but have different features. Compared with random selection, the selected core-set is both representative and diverse, with high information density.

Tab. 2. Evaluation metrics for Core-set and Random selection. A train set of 128 (12.5%) samples was selected to compare the performance of the core-set selection and randomly selection. W/ indicates nnU-Net was pre-trained on pseudo-labels before fine-tuning, while w/o means it was trained directly on the selected set without pre-training.

	Pre-trained	F1 score	Accuracy	Panoptic	Precision
Core-set	w/	0.6003	0.4291	0.5405	0.5045
Core-set	w/o	0.5939	0.4225	0.5342	0.4953
Random	w/	0.5773	0.4058	0.5173	0.4697
Random	w/o	0.5793	0.4076	0.5183	0.4732

samples). Fine-tuning surpasses pseudo-label-only pre-training (core-set = 0). *nnU-Net leverages pseudo-label pre-training for auto-configuration*.. As shown in Tab.1, coreset fine-tuned models consistently outperformed pseudo-label-only pre-trained models. *Core-set selection outperforms random selection*. Tab.2 shows that with 128 (12.5%) samples, the core-set improved F1 score, accuracy, panoptic, and precision, making core-set selection with pre-training the most effective for fine-tuning nnU-Net.

5 Discussion and conclusion

Pseudo-labels from CellSAM enable nnU-Net training without manual annotations. MicroSAM refines these labels semi-automatically, reducing effort. This pipeline integrates foundation models with traditional networks for efficient raw data use. Core-set fine-tuning surpasses pseudo-label pre-training and random selection.

In summary, this work presents an active learning workflow addressing two major pain-points in existing methods: (1) nnUnet requires considerable ground truth, but

6 Zhao, Zhou & Chen

usually not available in real applications, for auto-configuration, (2) foundation models cannot always provide completely satisfactory results off-the-shelf. The proposed framework seamlessly streamlines two powerful methods with minimal human intervention. Future work will enable continuous learning for dynamic datasets.

Disclaimer. The authors declare that there is no conflict of interest regarding the publication of this paper.

Acknowledgement. This work is supported by the by the Federal Ministry of Education and Research (BMBF) in Germany under the funding reference 161L0272, and also supported by the Ministry of Culture and Science (MKW) of the State of North Rhine-Westphalia.

References

- Ronneberger O, Fischer P, Brox T. U-net: Convolutional networks for biomedical image segmentation. 2015:234

 –41.
- Isensee F, Jaeger PF, Kohl SA, et al. nnU-Net: a self-configuring method for deep learningbased biomedical image segmentation. Nature methods. 2021;18(2):203–11.
- 3. Ash JT, Zhang C, Krishnamurthy A, et al. Deep batch active learning by diverse, uncertain gradient lower bounds. 2019.
- 4. Israel U, Marks M, Dilip R, et al. A foundation model for cell segmentation. bioRxiv: the preprint server for biology. 2024:2023–11.
- Yang L, Zhang Y, Chen J, et al. Suggestive annotation: A deep active learning framework for biomedical image segmentation. 2017:399–407.
- 6. He K, Chen X, Xie S, et al. Masked autoencoders are scalable vision learners. 2022:16000–9.
- Alexey D. An image is worth 16x16 words: Transformers for image recognition at scale. arXiv: 2010.11929, 2020.
- 8. Kirillov A, Mintun E, Ravi N, et al. Segment anything. 2023:4015–26.
- 9. Ravi N, Gabeur V, Hu YT, et al. Sam 2: Segment anything in images and videos. arXiv:2408.00714. 2024.
- 10. Archit A, Nair S, Khalid N, et al. Segment anything for microscopy. bioRxiv: the preprint server for biology. 2023:2023–8.
- 11. Ma J, He Y, Li F, et al. Segment anything in medical images. Nature Communications. 2024;15(1):654.
- Zha D, Bhat ZP, Lai KH, et al. Data-centric artificial intelligence: A survey. arXiv:2303.10158.
 2023.
- 13. Franco-Barranco D, Lin Z, Jang WD, et al. Current Progress and Challenges in Large-Scale 3D Mitochondria Instance Segmentation. IEEE transactions on medical imaging. 2023.
- 14. Zhou L, Liu H, Bae J, et al. Self pre-training with masked autoencoders for medical image classification and segmentation. 2023:1–6.
- 15. Wei D, Lin Z, Franco-Barranco D, et al. Mitoem dataset: Large-scale 3d mitochondria instance segmentation from em images. 2020:66–76.